Available online at www.sciencedirect.com
SCIENCE DIRECT®
International Journal of Mass Spectrometry 233 (2004) 293–298
International Journal of Mass Spectrometry
www.elsevier.com/locate/ijms

Calculations of electron-impact cross sections for the fragmentation and dissociative ionization of fullerenes using a semi-empirical method

P. Scheier [a,*], H. Deutsch [b], K. Becker [c], T.D. Märk [a,1]

[a] *Institut für Ionenphysik, Leopold-Franzens Universität, A-6020 Innsbruck, Austria*
[b] *Institut für Physik, Ernst-Moritz-Arndt Universität, D-17487 Greifswald, Germany*
[c] *Department of Physics and Center for Environmental Systems, Stevens Institute of Technology, Hoboken, NJ 07030, USA*

Received 1 December 2003; accepted 23 December 2003

Abstract

We extended our previously developed semi-empirical method for the calculation of cross section functions (absolute value and energy dependence) for the electron-impact ionization of the neutral fullerenes C_{60} and C_{70}, of the ionized fullerenes C_{60}^{z+} ($z = 1$–3), and of multiple ionization processes of the negatively charged fullerenes C_m^- ($m = 60$, 70, and 84) to the fragmentation and dissociative ionization of neutral and ionized C_{60} and C_{70}. Measured cross sections for these processes were found to display a sharp peak in the cross section function at low impact energies which was attributed to a plasmon excitation at these energies [Phys. Rev. Lett. 85 (2000) 3604], whereas the high-energy shape of the cross sections exhibited the well-known energy dependence of a direct ionization process. The introduction of a "decay factor" in our model allowed us to separate the two contributions and we found in all cases that the plasmon contribution to the cross section exhibits a very similar shape.

Keywords: Fullerenes; Ionization cross sections; Cluster; Electron impact

1. Introduction

Recently, we introduced a semi-empirical method for the calculation of absolute cross section functions for the electron-impact ionization of the neutral, positively, and negatively charged fullerenes C_{60} and C_{70} [1–3] which yielded results that were in general in good agreement with available experimental data [4–7]. Our method was initially developed for the calculation of partial cross section functions (absolute value and energy dependence) for the single electron-impact ionization of several neutral and ionized fullerenes C_{60}^{z+} ($z = 0$–3) [1]. Subsequently, we successfully extended this approach to the calculation of multiple electron-impact ionization cross sections of the neutral fullerenes C_{60} and C_{70} [2] and to the calculation of multiple electron-impact ionization cross sections of the negatively charged fullerenes C_m^- ($m = 60$, 70, 84) [3]. The necessity to rely on a semi-empirical approach to the calculation of electron-impact ionization cross section functions for neutral and ionized fullerenes that are in reasonably good agreement with experimentally determined cross sections [4–7] comes from the fact that more rigorous calculation methods [8–11], which yield reasonably good agreement (to within 20%) with measured data for a large number of simple as well as complex molecules, were not capable of reproducing the available experimental data for the fullerenes.

In the present paper, we extend the previous approach to the electron-impact induced fragmentation and dissociative ionization of neutral and ionized fullerenes, for which experimental data [4,12] consistently exhibit a very unusual and distinct cross section shape. Specifically, we consider the fragmentation of C_{60}^{z+} into C_{58}^{z+} ($z = 1$–3), the dissociative ionization of C_{60} into C_{58}^{z+} ($z = 1$–3), and dissociative ionization of C_{70} into C_n^+ ($n = 68, 66, 64, 62$). In the case of the electron induced fragmentation of C_{60}^+ the authors state [12] "At energies below 100 eV a well-pronounced peak-like structure can be observed and at higher energies the cross sections behave like a typical ionization cross section." In

* Corresponding author. Tel.: +43-512-507-6243; fax: +43-512-507-2932.
E-mail address: paul.scheier@uibk.ac.at (P. Scheier).
[1] Also Adjunct Professor: Department Plasma Physics, Comenius University, SK-84248 Bratislava, Slovakia.

1387-3806/$ – see front matter © 2004 Elsevier B.V. All rights reserved.
doi:10.1016/j.ijms.2003.12.034

an attempt to separate these two contributions, these authors fitted the high-energy part to a Lotz-formula [13]. They also proposed that the fragmentation process induced by electron impact at low energies is predominantly caused by a plasmon excitation. Here we extend our previously developed formalism in an effort to provide a description for the contributions to the measured cross sections arising from the direct ionization, which dominates at higher impact energies and, in the process, elucidate trends and similarities in the low-energy contributions attributed to plasmon excitation.

2. Background

In a previous paper [2] we introduced a general formula for the calculation of the partial ionization cross section $\sigma(C_m{}^{z+}, E)$ for the ionization of a fullerene C_m consisting of m monomers ($m = 60, 70$) to a final charge state z ($z =$ 1–6) as a function of the impact energy E of the form

$$\sigma(C_m{}^{z+}, E) = m^{2a} \cdot e^{-b_1} \cdot e^{-b_2} \cdot \sigma_C(E^*) \cdot F_{cage}(E) \quad (1)$$

with

$$E^* = E - [E_0 + (IP_{cluster-ion} - IP_{monomer})]$$
for ionic targets and multiple ionization of neutral fullerenes (2a)

$$E^* = E - E_0 \quad \text{for single ionization of neutral fullerenes} \quad (2b)$$

The exponent "a" (taken from Ref. [14]) results from a relationship between the radius of the cluster $R_{cluster}$ and the radius of the monomer $r_{monomer}$ of the form

$$R_{cluster} = m^a r_{monomer} \quad (3)$$

(see Ref. [15]), and the other quantities in formula (1) have the following meaning:

(i) The exponent "b_1" determines the so-called "structure factor", $\exp(-b_1)$. The structure factor leads to a reduction in the maximum fullerene ionization cross section compared to the value m^{2a} predicted by the simple "cluster" formula [14]. This is a consequence of the fact that fullerenes have very distinct structures that makes them different from simple collections of 60 or 70 independent C atoms. The exponent "b_1" was found to be a function of the cluster size "m" [2].

(ii) The exponent "b_2" determines the so-called "ionization factor", $\exp(-b_2)$. The ionization factor was found to decline exponentially for $z > 1$ for both C_{60} and C_{70} [2]and is different for fullerenes of different size m.

(iii) The energy dependence $F_{cage}(E)$ describes the deviation of the cross section shape of the fullerene C_m from the cross section shape of the monomer C. Different functions $F_{cage}(E)$ apply to C_{60} and C_{70} and to the various values of the final charge state z (see Ref. [2] for details).

(iv) The energy shift E^* as defined in Eqs. (2a) and (2b) was introduced as a way to properly describe the low energy dependence of the cross sections. Here E is the kinetic energy of the primary electron, and E_o describes the energy loss due to inelastic scattering. The values for the ionization energies (IPs) can be found in Ref. [6]. The combined effect of the function $F_{cage}(E)$ and the use of the "shifted" energy E^* in the monomer cross section is a shift of the maximum in the fullerene ionization cross section to higher energies in conjunction with a broadening of the region of the cross section maximum compared to the monomer ionization cross section and a more gradual decline of the fullerene cross section with increasing impact energy at higher impact energies (above about 100 eV).

(v) The quantity $\sigma_C(E^*)$ refers to the total ionization cross section of the carbon monomer as a function of the "shifted" energy E^* and is taken from the paper of Brook et al. [16].

The application of formula (1) required the empirical determination of the various parameters (structure factor, ionization factor, function $F_{cage}(E)$, and shifted energy E^*) from a sub-set of the measured experimental data [4–7] followed by the subsequent application of formula (1) to all cases for which experimental data are available. Further details can be found in our previous publications [1–3].

3. Extension of the formalism to the fragmentation and dissociative ionization of neutral and ionized fullerenes

In this section we describe in detail the extension of the DM formalism to three cases involving the fragmentation and dissociative ionization of neutral and ionized fullerenes. Specifically, we consider the fragmentation of $C_{60}{}^{z+}$ ($z =$ 1–3), the dissociative ionization of C_{60} into $C_{58}{}^{z+}$ ($z = 1$–3) fragment ions, and the dissociative ionization of C_{70} into $C_n{}^+$ ($n = 68, 66, 64, 62$) fragment ions.

3.1. Fragmentation of the fullerene ions $C_{60}{}^{z+}$ ($z = 1$–3) into $C_{58}{}^{z+}$ ions

The processes that we want to describe here are two-step processes of the form

$$C_{60}{}^+ + e^- \rightarrow C_{60}{}^{2+} + 2e^- \rightarrow C_{58}{}^+ + C_2 + e^- \quad (4a)$$

$$C_{60}{}^{2+} + e^- \rightarrow C_{60}{}^{3+} + 2e^- \rightarrow C_{58}{}^{2+} + C_2 + e^- \quad (4b)$$

$$C_{60}{}^{3+} + e^- \rightarrow C_{60}{}^{4+} + 2e^- \rightarrow C_{58}{}^{3+} + C_2 + e^- \quad (4c)$$

where, for example in (4a), the initial direct ionization is followed by the recapture of one of the two outgoing electrons, which subsequently induces the fragmentation of the doubly charged fullerene into a singly charged fragment ion

Table 1
Summary of pertinent parameters required for the application of Eqs. (5), (7) and (9)

Process	Parameter b_2	Parameter E_o	Parameter F_{decay}
$C_{60}^+ \rightarrow C_{58}^+$	0.255	35 eV	0.132
$C_{60}^{2+} \rightarrow C_{58}^{2+}$	0.510	35 eV	0.255
$C_{60}^{3+} \rightarrow C_{58}^{3+}$	0.765	35 eV	0.500
$C_{60} \rightarrow C_{58}^+$	1.347	75 eV	0.046
$C_{60} \rightarrow C_{58}^{2+}$	3.442	90 eV	0.55
$C_{60} \rightarrow C_{58}^{3+}$	5.438	115 eV	1.0
$C_{70} \rightarrow C_{68}^+$	0.693	75 V	0.02241
$C_{70} \rightarrow C_{66}^+$	0.693	80 V	0.01259
$C_{70} \rightarrow C_{64}^+$	0.693	85 eV	0.00720
$C_{70} \rightarrow C_{62}^+$	0.693	90 eV	0.00145

Listed are the ionization factor "b_2", the energy parameter E_0, and the decay factor F_{decay}. For the processes studied here. All other parameters can be found in our earlier publications [1–3].

and a neutral C_2 molecule. We modify the above Eq. (1) in an effort to describe the contributions to the above processes attributable to the direct ionization and write it in the following form:

$$\sigma(C_{60}^{z+}, E) = (60)^{0.768} \cdot e^{-0.79} \cdot e^{-b_2} \cdot \sigma_C(E^*) \cdot F_{cage}(E) \cdot F_{decay} \quad (5)$$

where we introduced a "fragmentation factor" F_{decay} in an effort to separate the two contributions to the measured cross section, the low-energy contribution attributed to plasmon excitation and the high-energy direct ionization part. The fragmentation factors F_{decay} were determined empirically from a fit of the cross section described by Eq. (5) and the experimental data [12], all other required parameters were taken from Refs. [1–3] using $E_0 = 35$ eV. The pertinent parameters are also summarized in Table 1 (together with the values of these parameters that are required for the cross section calculations of the processes discussed below).

3.2. Dissociative ionization of C_{60} into C_{58}^{z+} (z = 1–3) fragment ions

We now consider the dissociative ionization of the neutral fullerenes C_{60} into C_{58}^{z+} (z = 1–3) fragment ions. As before, we view the process as a two-step reaction of the form

$$C_{60}^+ + e^- \rightarrow C_{60}^{(z+1)} + (z+2)e^- \rightarrow C_{58}^{z+} + (z+1)e^- \quad (6)$$

(z = 1–3) where a $(z+1)$-fold positively charged parent ion is initially produced, which subsequently dissociates into a C_{58}^{z+} fragment ion accompanied by the recapture of one of the outgoing electrons. Our formalism yields the following expression

$$\sigma(C_{60}^{z+}, E) = (60)^{0.768} \cdot e^{-0.79} \cdot e^{-b_2} \cdot \sigma_C(E^*) \cdot F_{cage}(E) \cdot F_{decay} \quad (7)$$

with $E^* = E_o - E$. Eq. (7) is formally identical to Eq. (5), but the specific values of E^*, $F_{cage}(E)$, and F_{decay} depend on the charge state "z". The values of E_o (which determines E^*) and F_{decay}, which were obtained empirically, are summarized in Table 1 and the function $F_{cage}(E)$ is taken from Ref. [2].

3.3. Dissociative ionization of C_{70} into C_n^+ (n = 68, 66, 64, 62) fragment ions

The dissociative ionization of C_{70} into singly charged C_n^+ (n = 68, 66, 64, 62) fragment ions

$$C_{70} + e^- \rightarrow C_{70}^{2+} + 3e^- \rightarrow C_{70-iC_2}^+ + iC_2 + 2e^- \quad (8)$$

(i = 1–4 for C_{68}^+, C_{66}^+, C_{64}^+, and C_{62}^+) is considered next. Here, a doubly charged parent ion is initially produced, which subsequently dissociates accompanied by the recapture of one of the outgoing electrons. Our formalism applied yields the following expression

$$\sigma(C_{60}, E) = (70)^{0.768} \cdot e^{-1.132} \cdot e^{-0.693} \cdot \sigma_C(E^*) \cdot F_{cage}(E) \cdot F_{decay} \quad (9)$$

with $E^* = E_o - E$ where the pertinent values E_o and F_{decay}, which were determined empirically, are listed in Table 1 and F_{cage} is taken from Ref. [2].

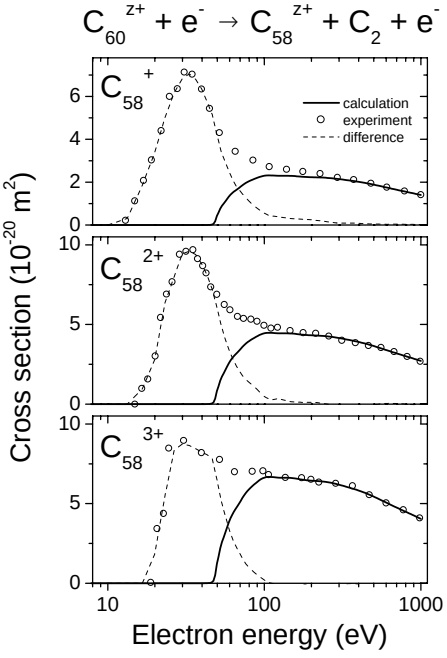

Fig. 1. Cross section for the fragmentation of C_{60}^{z+} into C_{58}^{z+} (z = 1–3) as a function of electron energy. The measured data (open circles) are compared with the present calculation (solid line). Also shown is the difference (dashed line) between the measured data and the present calculation which is attributed to the plasmon contribution in the process (see text for details).

4. Results and discussion

Fig. 1 shows the measured cross sections for the two-step fragmentation of C_{60}^{z+} ($z = 1$–3) into C_{58}^{z+} from Ref. [12] via the processes (4a) through (4c) in comparison with our calculation, which describes only the direct ionization part of the process. Also shown is the difference between the measured and the calculated data, which represents the contribution attributed to plasmon excitation. In all three cases, the plasmon part has a prominent maximum around 30 eV and decreases rapidly with increasing impact energy and above 100 eV, the direct ionization part dominates the cross section. Two observations are noteworthy, (i) the ratio of the peak heights of the plasmon part to the direct ionization part decreases with increasing charge state of the target and (ii) the threshold for the three curves shifts slightly towards higher impact energy as the charge state of the target increases.

Fig. 2 shows similar curves for the dissociative ionization of C_{70} into C_m^+ fragments ($m = 68, 66, 64, 62$) via processes (8). Again, the plasmon contribution shows a sharp peak at low energy and becomes essentially negligible at energies above about 150 eV. Here, the ratio of the peak heights of the plasmon contribution to the direct ionization contribution stays essentially constant at a value of about 3. As expected, the plasmon contribution shifts slightly towards higher impact energies as the number of C_2 fragments produced in the process increases.

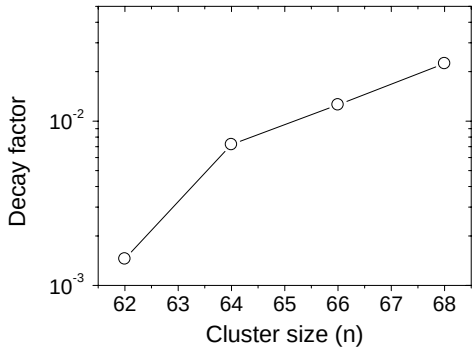

Fig. 3. Decay factor for the dissociative ionization of C_{70} into C_n^+ as a function of cluster size n.

Fig. 3 shows the decay factor as a function of the cluster size. It is apparent that the decay factor and thus the absolute values of the ionization cross section declines as the number of C_2 dimes produced in the process increases.

Fig. 4 shows the measured cross sections for the two-step dissociative ionization of C_{60} into C_{58}^{z+} ($z = 1$–3) from Ref. [12] via the process (4) in comparison with our calculation, which describes only the direct ionization part of the process. Also shown is the difference between the mea-

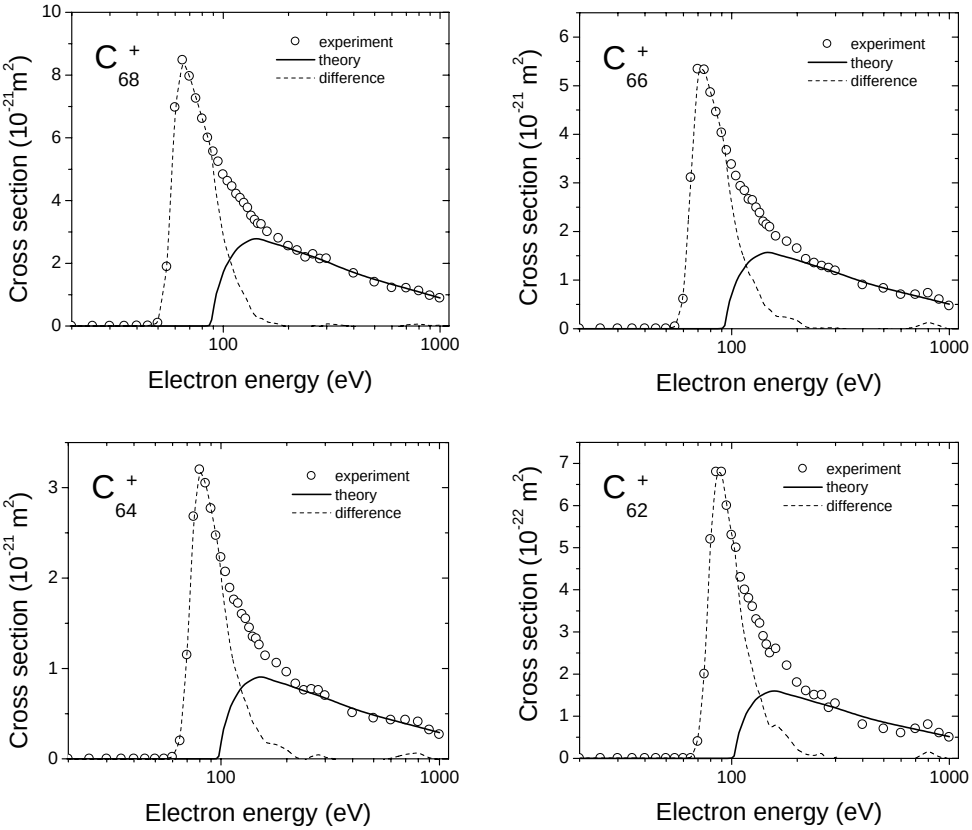

Fig. 2. Cross section for the dissociative ionization of C_{70} as a function of electron energy. The measured data (open circles) are compared with the present calculation (solid line). Also shown is the difference (dashed line) between the measured data and the present calculation which is attributed to the plasmon contribution in the process (see text for details).

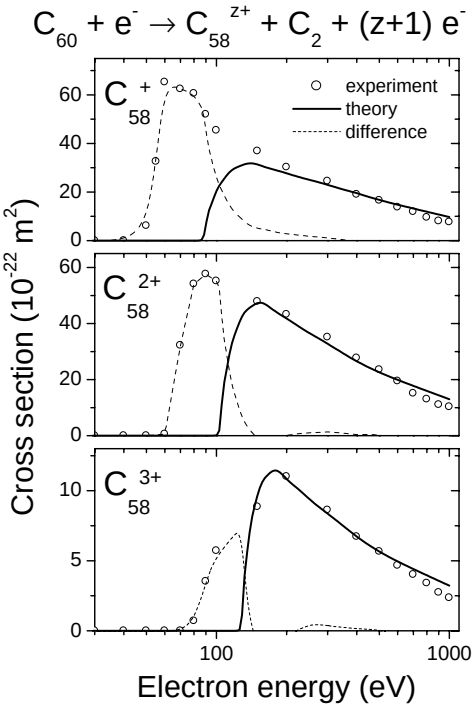

Fig. 4. Cross section for the dissociative ionization of C_{60} as a function of electron energy. The measured data (open circles) are compared with the present calculation (solid line). Also shown is the difference (dashed line) between the measured data and the present calculation which is attributed to the plasmon contribution in the process (see text for details).

sured and the calculated data, which represents the contribution attributed to plasmon excitation. The magnitude of the plasmon part relative to the direct ionization part decreases sharply with increasing charge state of the C_{58} fragment ion. Furthermore, the position of the threshold of the plasmon contribution and the energy at which it peaks shift to higher energies as the charge state of the fragment ion increases as one would expect.

Fig. 5 shows the decay factor as a function of the charge state for both the ions and the neutrals. As one would expect, the decay factor is different for ions and neutrals and exhibits a behavior that indicates that the fragmentation of a high-z target is more efficient, i.e., has a higher cross section.

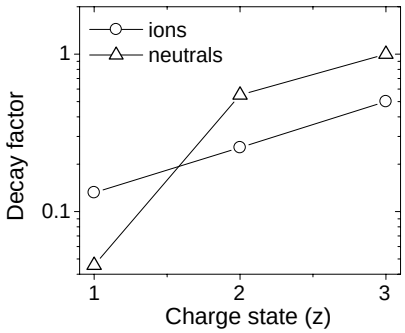

Fig. 5. Decay factor for the fragmentation of C_{60}^{z+} into $C_{58}^{z+} + C_2$ ($z = 1$–3) and for the dissociative ionization of C_{60} into C_{58}^{z+} ($z = 1$–3) as a function of the charge state.

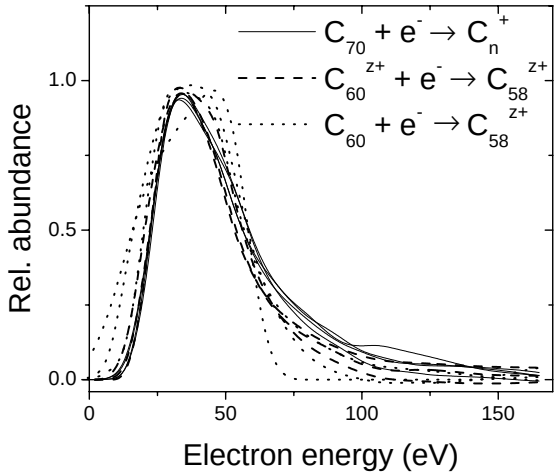

Fig. 6. Plasmon contribution as a function of electron energy for the fragmentation of C_{60}^{z+} ($z = 1$–3) ions (dashed lines), the dissociative ionization of C_{60} into C_{58}^{z+} ($z = 1$–3) (dotted lines), and the dissociative ionization of C_{70} into C_n^+ ($n = 68$, 66, 64, 62) (solid lines). The various curves are labeled in the figure. All curves have been normalized to the same peak height and have been shifted in energy to the energy position of the pure fragmentation process.

Lastly, Fig. 6 shows the plasmon contributions extracted from the various measured data shown in Figs. 1, 2 and 4. The various contributions have all been normalized in terms of their absolute magnitude in order to facilitate a meaningful comparison. Furthermore, the plasmon contributions extracted from the dissociative ionization processes have been shifted to the energy position of pure fragmentation. The various curves displayed in Fig. 6 show a very similar behavior, a sharp peak around 30 eV and a rapid drop above 50 eV, which indicates (i) that the plasmon contribution exhibits an almost resonance-like energy dependence and (ii) that the processes studied here are dominated by direct ionization at energies above about 100 eV.

5. Conclusions

We extended our semi-empirical method for the calculation of cross section functions (absolute value and energy dependence) for the electron-impact ionization of the neutral fullerenes C_{60} and C_{70}, of the ionized fullerenes C_{60}^{z+} ($z = 1$–3), and of multiple ionization processes of the negatively charged fullerenes C_m^- ($m = 60$, 70, and 84) to the fragmentation and dissociative ionization of neutral and ionized C_{60} and C_{70}. Measured cross sections for these processes display a sharp peak in the cross section function at low impact energies which was attributed to a plasmon excitation at these energies [7], whereas the high-energy shape of the cross sections exhibit the well-known energy dependence of a direct ionization process. The introduction of a “decay factor” in our model allowed us to separate the two contributions and we found

in all cases that the plasmon contribution to the cross section exhibits a very similar shape and the high-energy part of the cross section was dominated by direct ionization.

Acknowledgements

This work was partially supported by the Österreichischer Fonds zur Förderung der Wissenschaftlichen Forschung, Wien, Austria and the EU Commission network programme, Brussels. One of us (K.B.) wishes to acknowledge partial financial support from the U.S. Department of Energy, Office of Science.

References

[1] H. Deutsch, P. Scheier, K. Becker, T.D. Märk, Int. J. Mass Spectrom. 223/224 (2003) 1.
[2] H. Deutsch, P. Scheier, K. Becker, T.D. Märk, Int. J. Mass Spectrom. 223/224 (2003) 253.
[3] P. Scheier, H. Deutsch, K. Becker, T.D. Märk, Int. J. Mass Spectrom. 223/224 (2003) 703.
[4] S. Matt, B. Dünser, M. Lezius, H. Deutsch, K. Becker, A. Stamatovic, P. Scheier, T.D. Märk, J. Chem. Phys. 105 (1996) 1880.
[5] R. Völpel, G. Hofmann, M. Steidl, M. Stenke, M. Schlapp, R. Trassl, E. Salzborn, Phys. Rev. Lett. 71 (1993) 3439.
[6] S. Matt, O. Echt, R. Wörgötter, V. Grill, P. Scheier, C. Lifshitz, T.D. Märk, Chem. Phys. Lett. 264 (1997) 149.
[7] D. Hathiramani, P. Scheier, K. Aichele, K. Huber, E. Salzborn, Chem. Phys. Lett. 319 (2000) 13.
[8] Y.-K. Kim, M.E. Rudd, Phys. Rev. A 50 (1994) 3954.
[9] W. Hwang, Y.-K. Kim, M.E. Rudd, J. Chem. Phys. 104 (1996) 2956.
[10] H. Deutsch, K. Becker, S. Matt, T.D. Märk, Int. J. Mass Spectrom. 197 (2000) 37.
[11] S. Keller, E. Engel, Chem. Phys. Lett. 299 (1999) 165.
[12] D. Hathiramani, K. Aichele, W. Arnold, K. Huber, E. Salzborn, P. Scheier, Phys. Rev. Lett. 85 (2000) 3604.
[13] W. Lotz, Z. Phys. 206 (1967) 205.
[14] H. Deutsch, K. Becker, T.D. Märk, Eur. Phys. J. D 12 (2000) 283.
[15] H. Deutsch, K. Becker, T.D. Märk, Int. J. Mass Spectrom. Ion Proc. 144 (1995) L9.
[16] E. Brook, M.F.A. Harrison, A.C.H. Smith, J. Phys. B 11 (1978) 3115.